

Quantitative homogenization on percolation clusters and interacting particle systems

Chenlin Gu

DMA/ENS, PSL Research University

Ph.D. Defense

April 1st, 2021

Homogenization

- Elliptic Dirichlet problem with random coefficient in a large domain

$$\begin{cases} -\nabla \cdot (\mathbf{a} \nabla u) = f & \text{in } Q_r, \\ u = g & \text{on } \partial Q_r. \end{cases}$$

- $\mathbf{a} : \mathbb{R}^d \rightarrow \mathbb{R}^{d \times d}$ **random coefficient**:
 - symmetric;
 - \mathbb{Z}^d -stationary and ergodic;
 - uniform ellipticity, i.e. there exists $\Lambda > 1$ such that for any $x \in \mathbb{R}^d$, $|\xi|^2 \leq \xi \cdot \mathbf{a}(x) \xi \leq \Lambda |\xi|^2$.
- $Q_r := \left(-\frac{r}{2}, \frac{r}{2}\right)^d$, $g, f \in H^1(Q_r)$.

Homogenization

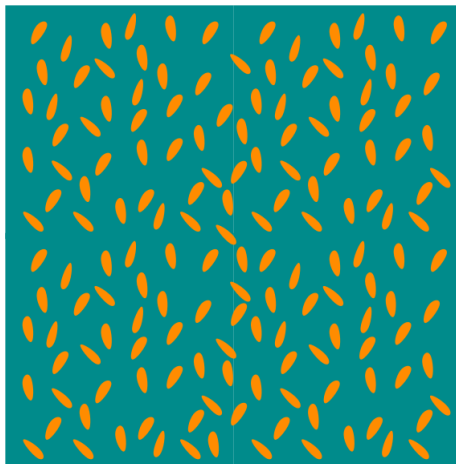


Figure: An illustration of random coefficient.

Homogenization

- Elliptic Dirichlet problem with random coefficient in a large domain

$$\begin{cases} -\nabla \cdot (\mathbf{a} \nabla u) = f & \text{in } Q_r, \\ u = g & \text{on } \partial Q_r. \end{cases}$$

- For very large r , the solution can be approximated by the homogenized solution \bar{u} for

$$\begin{cases} -\nabla \cdot (\bar{\mathbf{a}} \nabla \bar{u}) = f & \text{in } Q_r, \\ \bar{u} = g & \text{on } \partial Q_r, \end{cases}$$

where $\bar{\mathbf{a}} \in \mathbb{R}^{d \times d}$ is the (deterministic) effective coefficient.

- Generally, $\bar{\mathbf{a}} \neq \mathbb{E}[\mathbf{a}]$.

Historical results

- Qualitative homogenization: 1970-2000.
- Quantitative homogenization: 2000-present.



Figure: Some researchers who contribute to homogenization theory: Alain Bensoussan, Jacques-Louis Lions, George Papanicolaou, Ennio De Giorgi, François Murat, Luc Tartar, Thomas Spencer, S. R. Srinivasa Varadhan, Grégoire Allaire, Marco Avellaneda, Carlos Kenig, Fanghua Lin, Zhongwen Shen, Felix Otto, Antoine Gloria, Stefan Neukamm, Scott Armstrong, Charles Smart, Jean-Christophe Mourrat, Tuomo Kuusi, Arianna Giunti.

Table of Contents

- 1 Homogenization and numerical algorithm
- 2 Homogenization on percolation clusters
- 3 Homogenization for interacting particle systems

Outline

- 1 Homogenization and numerical algorithm
- 2 Homogenization on percolation clusters
- 3 Homogenization for interacting particle systems

Numerical methods

- Elliptic Dirichlet problem with random coefficient in a large domain

$$\begin{cases} -\nabla \cdot (\mathbf{a} \nabla u) = f & \text{in } Q_r, \\ u = g & \text{on } \partial Q_r. \end{cases}$$

- Some classical methods to solve this problem:

- Jacobi iterative method;
- Multigrid method;
- Homogenization.

Classical methods

Jacobi iteration

- Jacobi iterative method = iteration of semigroup.
- After discretization,
 $P(x, y) := \frac{\mathbf{a}(x, y)}{\sum_{z \sim x} \mathbf{a}(x, z)}, \tilde{f}(x) = f(x) / (\sum_{z \sim x} \mathbf{a}(x, z)).$
- We do iteration $u_0 = g, u_{n+1} = J(u_n, \tilde{f})$

$$J(u_n, \tilde{f}) := Pu_n + \tilde{f}.$$

-
- u is the unique solution of the equation $u = Pu + \tilde{f}, \lim_{n \rightarrow \infty} u_n = u$.
 - **Advantages:** Easy to program and converges exponentially.
 - **Disadvantages:** The contraction rate of one iteration is $(1 - \frac{1}{r^2})$, so at least $O(r^2)$ iterations and takes time for large r .

Classical methods

Multigrid method

Efficient method for $\mathbf{a} \equiv const.$ i.e. for the problem $-\Delta u = f$.

- ① Try to solve $-\Delta u = f$, we do the Jacobi iteration and $u_1 = J^M(u_0, f)$.
- ② $f_1 = f - (-\Delta u_1)$, coarsen the grid by 2, and $u_2 = J^{M/2}(0, f_1)$.
- ③ $f_2 = f_1 - (-\Delta u_2)$, coarsen the grid by 2, and $u_3 = J^{M/4}(0, f_2)$.
- ④ $\hat{u} = u_1 + u_2 + u_3$. Iterate this procedure.

Multigrid method

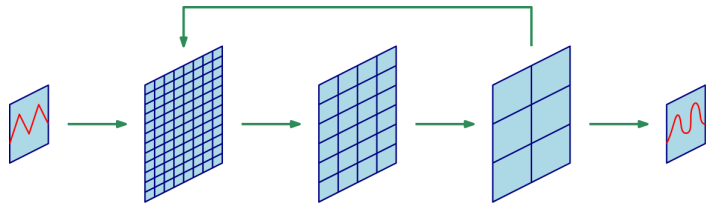


Figure: An illustration for the procedures of multigrid algorithm.

- Probabilistic interpretation: coarsened grid \approx random walk with big step size.
- **Advantages:** Only $O(\log(r))$ iterations are required in Q_r .
- **Disadvantages:** a has to be constant.

Classical methods

Homogenized solution

- Solve the homogenized solution \bar{u} instead of u

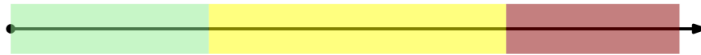
$$\begin{cases} -\nabla \cdot (\bar{\mathbf{a}} \nabla \bar{u}) = f & \text{in } Q_r, \\ \bar{u} = g & \text{on } \partial Q_r. \end{cases}$$

- Because $\bar{\mathbf{a}}$ is constant, the multigrid algorithm works.
- Remark:** $\bar{\mathbf{a}} \neq \mathbb{E}[\mathbf{a}]$ and can be solved much more quickly.
- Advantages:** It is as fast as multigrid method.
- Disadvantages:**
 - For r fixed, there is always a difference between u and \bar{u} .
 - Loss of local details: u and \bar{u} is only close in L^2 .

Beyond homogenized solution

- **Question:** A precision beyond the limit of homogenization.

For r big, and for a high precision ???



Small r
a naive Jacobi iteration.

Very very big r
beyond the capacity of mesh.
homogenized solution + multigrid.

Main result 1: AHKM algorithm

Armstrong, Hannukainen, Kuusi, Mourrat 18

- Initial guess $u_0 := g$.
- Solve the following equations with the null Dirichlet boundary condition:

$$\begin{cases} (\lambda^2 - \nabla \cdot \mathbf{a} \nabla) u_1 &= f + \nabla \cdot \mathbf{a} \nabla u_0 & \text{in } Q_r, \\ -\nabla \cdot \bar{\mathbf{a}} \nabla \bar{u} &= \lambda^2 u_1 & \text{in } Q_r, \\ (\lambda^2 - \nabla \cdot \mathbf{a} \nabla) u_2 &= (\lambda^2 - \nabla \cdot \bar{\mathbf{a}} \nabla) \bar{u} & \text{in } Q_r. \end{cases}$$

- $\hat{u} := u_0 + u_1 + u_2$ and we put \hat{u} in the place of u_0 to restart the iteration.

Main result 1: AHKM algorithm

Theorem (Gu 2018, Gu 2019)

With high probability, the AHKM algorithm converges in $H^1(Q_r)$ to the original solution u of the Dirichlet problem, with a similar complexity as the homogenized solution \bar{u} . It also applies to the percolation cluster setting.

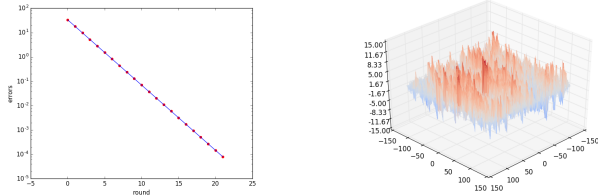


Figure: The image on the left shows the convergence of the AHKM algorithm. The image on the right illustrates the corrector on the maximal cluster of a cube 256×256 .

Proof: Two-scale expansion

- AHKM algorithm

$$\implies \begin{cases} -\nabla \cdot \mathbf{a} \nabla (u - u_0 - u_1) &= -\nabla \cdot \bar{\mathbf{a}} \nabla \bar{u} & \text{in } Q_r, \\ (\lambda^2 - \nabla \cdot \mathbf{a} \nabla) u_2 &= (\lambda^2 - \nabla \cdot \bar{\mathbf{a}} \nabla) \bar{u} & \text{in } Q_r. \end{cases}$$

- First order corrector $\{\phi_{e_k}\}_{1 \leq k \leq d}$: $-\nabla \cdot \mathbf{a}(e_k + \nabla \phi_{e_k}) = 0$ in \mathbb{R}^d .
- Two-scale expansion $w := \bar{u} + \sum_{k=1}^d (\partial_{e_k} \bar{u}) \phi_{e_k}$.
- $|\hat{u} - u| = |u - (u_0 + u_1 + u_2)| \leq |(u - u_0 - u_1) - w| + |w - u_2|$, so it reduces to the quantitative estimate of two-scale expansion.

Outline

- 1 Homogenization and numerical algorithm
- 2 Homogenization on percolation clusters
- 3 Homogenization for interacting particle systems

Bernoulli percolation on \mathbb{Z}^d

- (\mathbb{Z}^d, E_d) : d -dimensional lattice graph.
- $\{\mathbf{a}(e)\}_{e \in E_d}$ i.i.d. random variables of Bernoulli law

$$\mathbb{P}[\mathbf{a}(e) = 1] = p, \quad \mathbb{P}[\mathbf{a}(e) = 0] = 1 - p.$$

- $\mathbf{a}(e) = 1 \Leftrightarrow e$ is open; $\mathbf{a}(e) = 0 \Leftrightarrow e$ is closed.
- A connected component given by the open edges will be called cluster.
- $\theta(p) := \mathbb{P}[0 \text{ belongs to an infinite cluster } \mathcal{C}_\infty]$.
- For $d \geq 2$, there exists a critical point

$$p_c := \inf\{p \in [0, 1] : \theta(p) > 0\} \in (0, 1).$$

- Phase transition: for $d \geq 2$
 - Subcritical: $p \in (0, p_c)$, no infinite cluster \mathcal{C}_∞ , $\theta(p) = 0$;
 - Supercritical: $p \in (p_c, 1]$, a unique infinite cluster \mathcal{C}_∞ , $\theta(p) \in (0, 1]$;
 - Critical: $\theta(p_c) = 0$ is still open for $3 \leq d \leq 10$.

Infinite cluster \mathcal{C}_∞ in supercritical percolation

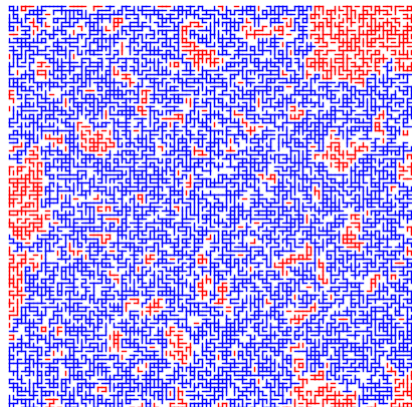
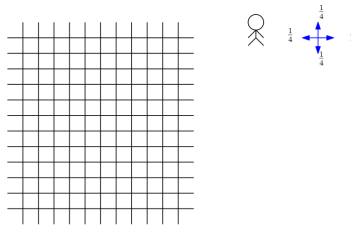


Figure: The cluster in blue is the maximal cluster in the cube.

Universality of Brownian motion

- It is well-known that a centered random walk $(S_n)_{n \geq 1}$ on \mathbb{Z}^d with variance σ^2 converge to the Brownian motion $(\sigma B_t)_{t \geq 0}$ after a scaling.



- From different viewpoints: CLT, local CLT, invariance principle.
- Question:** Do these results also hold for the random walk in suitable random environment?

Random walk on the infinite cluster

- We focus on the case **supercritical** percolation.
- (X_t) is a continuous-time **Markov jump process** starting from $y \in \mathcal{C}_\infty$, with an associated generator

$$\nabla \cdot \mathbf{a} \nabla u(x) := \sum_{z \sim x} \mathbf{a}(\{x, z\}) (u(z) - u(x)).$$

- The **quenched semigroup** is defined as

$$p(t, x, y) = p^{\mathbf{a}}(t, x, y) := \mathbb{P}_y^{\mathbf{a}}(X_t = x),$$

which also solves the equation on \mathcal{C}_∞ that

$$\begin{cases} \partial_t p(t, \cdot, y) - \nabla \cdot \mathbf{a} \nabla p(t, \cdot, y) = 0 & , \\ p(0, \cdot, y) = \delta_y(\cdot) & . \end{cases}$$

Random walk on the infinite cluster

- Previous work: Invariance principle by Vladas Sidoravicius, Alain-Sol Sznitman, Marek Biskup, Noam Berger, Pierre Mathieu, Andrey Piatnitski, Gaussian bound for $p(t, x, y)$ by Martin Barlow, and asymptotic local CLT by Martin Barlow and Ben Hambly.



Figure: From left to right is Vladas Sidoravicius, Alain-Sol Sznitman, Marek Biskup, Noam Berger, Pierre Mathieu, Andrey Piatnitski, Martin Barlow, Ben Hambly.

Semigroup of random walk on \mathcal{C}_∞

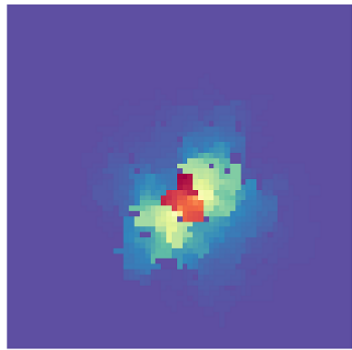


Figure: An illustration of $t^{\frac{d}{2}} p(t, \cdot, 0)$ for $t = 100$.

Semigroup of random walk on \mathcal{C}_∞

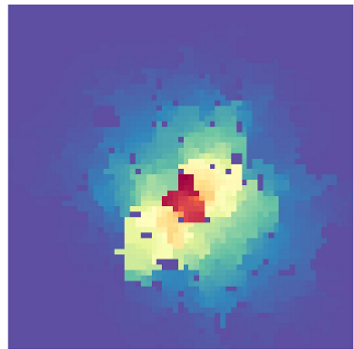


Figure: An illustration of $t^{\frac{d}{2}} p(t, \cdot, 0)$ for $t = 200$.

Semigroup of random walk on \mathcal{C}_∞

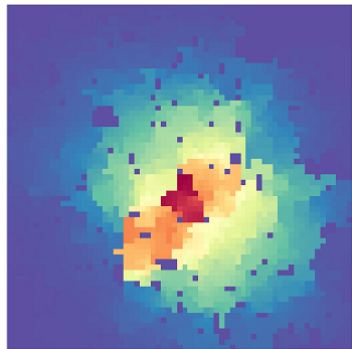


Figure: An illustration of $t^{\frac{d}{2}} p(t, \cdot, 0)$ for $t = 300$.

Semigroup of random walk on \mathcal{C}_∞

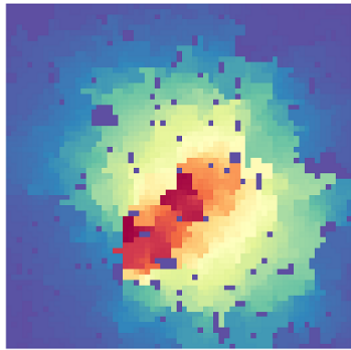


Figure: An illustration of $t^{\frac{d}{2}} p(t, \cdot, 0)$ for $t = 400$.

Semigroup of random walk on \mathcal{C}_∞

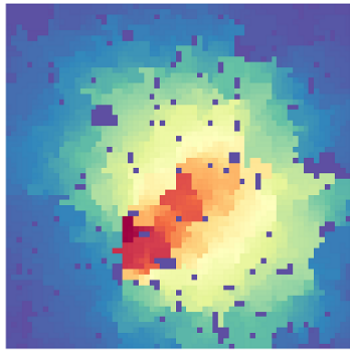


Figure: An illustration of $t^{\frac{d}{2}} p(t, \cdot, 0)$ for $t = 500$.

Semigroup of random walk on \mathcal{C}_∞

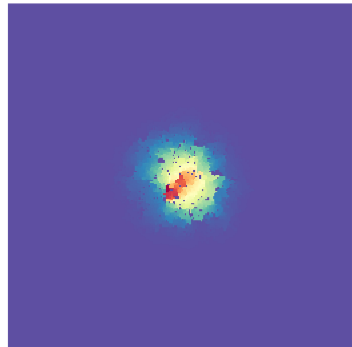


Figure: An illustration of $t^{\frac{d}{2}} p(t, \cdot, 0)$ for $t = 500$.

Semigroup of random walk on \mathcal{C}_∞

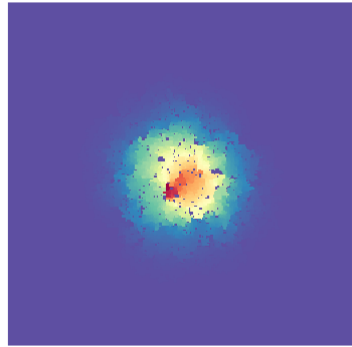


Figure: An illustration of $t^{\frac{d}{2}} p(t, \cdot, 0)$ for $t = 1000$.

Semigroup of random walk on \mathcal{C}_∞

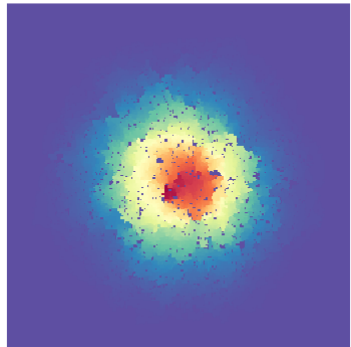


Figure: An illustration of $t^{\frac{d}{2}} p(t, \cdot, 0)$ for $t = 2000$.

Semigroup of random walk on \mathcal{C}_∞

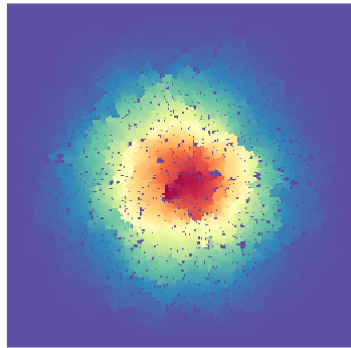


Figure: An illustration of $t^{\frac{d}{2}} p(t, \cdot, 0)$ for $t = 3000$.

Semigroup of random walk on \mathcal{C}_∞

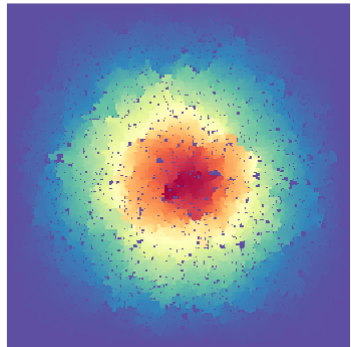


Figure: An illustration of $t^{\frac{d}{2}} p(t, \cdot, 0)$ for $t = 4000$.

Main result 2: Quantitative local CLT

Theorem (Dario, Gu, AOP 2021)

For each exponent $\delta > 0$, there exist a positive constant $C(d, \mathfrak{p}, \delta) < \infty$ and an exponent $s(d, \mathfrak{p}, \delta) > 0$, such that for every $y \in \mathbb{Z}^d$, there exists a non-negative random time $\mathcal{T}_{\text{par},\delta}(y)$ satisfying the stochastic integrability estimate

$$\forall T \geq 0, \quad \mathbb{P}(\mathcal{T}_{\text{par},\delta}(y) \geq T) \leq C \exp\left(-\frac{T^s}{C}\right),$$

such that, on the event $\{y \in \mathcal{C}_\infty\}$, for every $x \in \mathcal{C}_\infty$ and every $t \geq \max(\mathcal{T}_{\text{par},\delta}(y), |x - y|)$,

$$|p(t, x, y) - \theta(\mathfrak{p})^{-1} \bar{p}(t, x - y)| \leq Ct^{-\frac{d}{2} - (\frac{1}{2} - \delta)} \exp\left(-\frac{|x - y|^2}{Ct}\right).$$

Remark: $\theta(\mathfrak{p}) = \mathbb{P}[0 \in \mathcal{C}_\infty]$ is the factor of the density normalization.
 $(\bar{p}(t, \cdot - y))_{t \geq 0}$ is the semigroup of the limit Brownian motion $(\sigma B_t)_{t \geq 0}$.

Errors between the semigroups

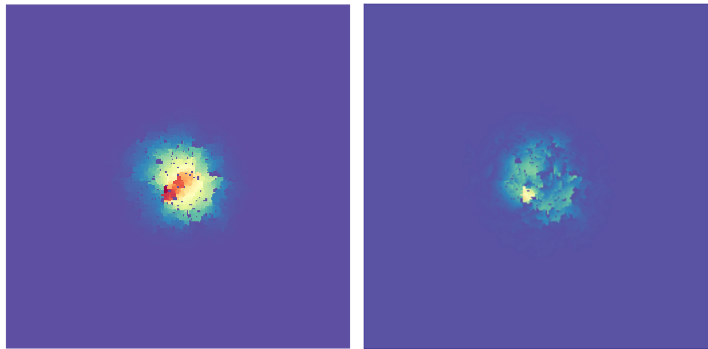


Figure: $t = 500$, the image on the left: $t^{\frac{d}{2}} p(t, \cdot, 0)$;
the image on the right: $t^{\frac{d}{2}} |p(t, \cdot, 0) - \theta(\mathfrak{p})^{-1} \bar{p}(t, \cdot)|$.

Errors between the semigroups

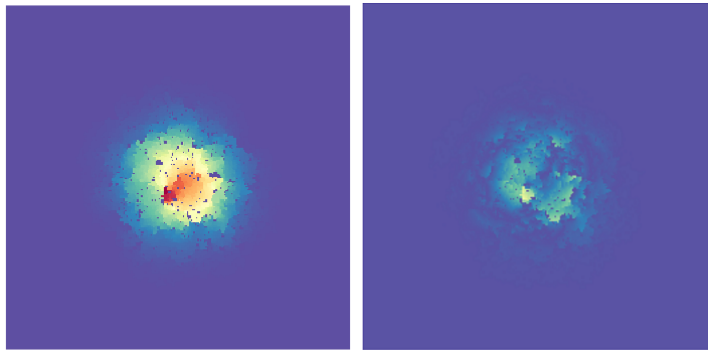


Figure: $t = 1000$, the image on the left: $t^{\frac{d}{2}} p(t, \cdot, 0)$;
the image on the right: $t^{\frac{d}{2}} |p(t, \cdot, 0) - \theta(\mathfrak{p})^{-1} \bar{p}(t, \cdot)|$.

Errors between the semigroups

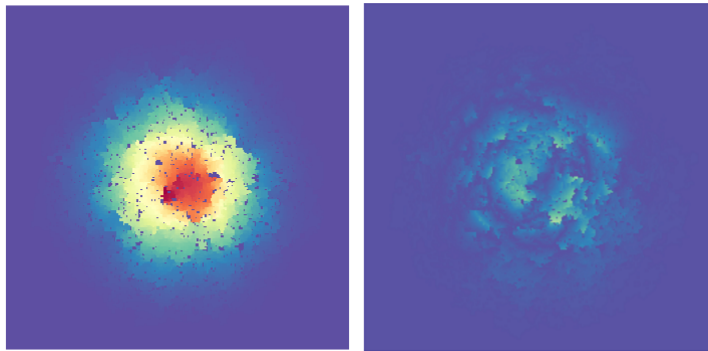


Figure: $t = 2000$, the image on the left: $t^{\frac{d}{2}} p(t, \cdot, 0)$;
the image on the right: $t^{\frac{d}{2}} |p(t, \cdot, 0) - \theta(\mathfrak{p})^{-1} \bar{p}(t, \cdot)|$.

Errors between the semigroups

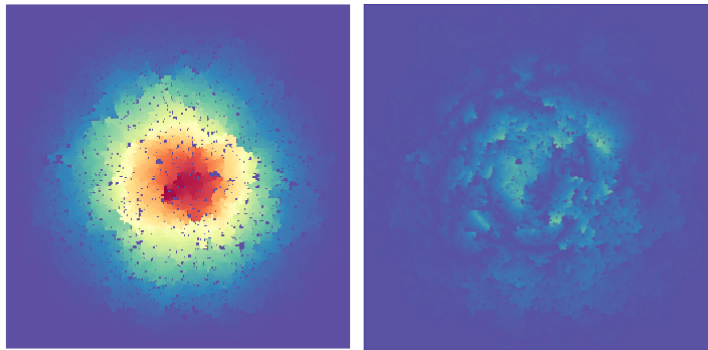


Figure: $t = 3000$, the image on the left: $t^{\frac{d}{2}} p(t, \cdot, 0)$;
the image on the right: $t^{\frac{d}{2}} |p(t, \cdot, 0) - \theta(\mathfrak{p})^{-1} \bar{p}(t, \cdot)|$.

Errors between the semigroups

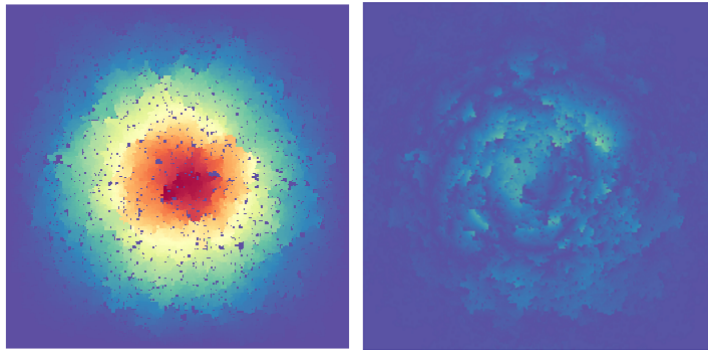


Figure: $t = 4000$, the image on the left: $t^{\frac{d}{2}} p(t, \cdot, 0)$;
the image on the right: $t^{\frac{d}{2}} |p(t, \cdot, 0) - \theta(\mathfrak{p})^{-1} \bar{p}(t, \cdot)|$.

Proof: Partition of good cube

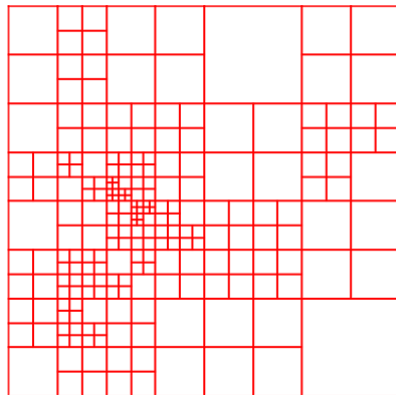


Figure: An illustration of Calderón-Zygmund decomposition.

Proof: Partition of good cube

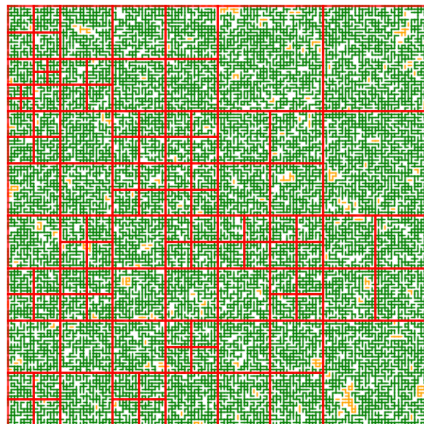


Figure: Strategy from Armstrong-Dario 18, partition \mathbb{Z}^d into of disjoint small cubes such that 1, every cube has good property; 2, every cube is not large with high probability; 3, every neighbor cube has comparable size.

Outline

- 1 Homogenization and numerical algorithm
- 2 Homogenization on percolation clusters
- 3 Homogenization for interacting particle systems

Interacting particle systems



Figure: Some researchers who contribute to interacting particle systems: George Papanicolaou, S. R. Srinivasa Varadhan, Herbert Spohn, Claude Kipnis, Claudio Landim, Horng-Tzer Yau, Tadahisa Funaki, Stefano Olla, Jeremy Quastel, Milton Jara, Patricia Gonçalves, François Golse, Sylvia Serfaty, Isabelle Gallagher, Laure Saint-Raymond, Thierry Bodineau.

Interacting particle systems

Example: Generalized symmetric exclusion process

- Configuration $\eta : \mathbb{Z}^d \rightarrow \{0, 1, \dots, \kappa\}$, $\kappa \geq 2$.
- Generator $\mathcal{L}f(\eta) = \frac{1}{2} \sum_{x \in \mathbb{Z}^d} \sum_{y \sim x} \mathbf{1}_{\{\eta(x) > 0, \eta(y) < \kappa\}} (f(\eta^{x,y}) - f(\eta))$,

with

$$\eta^{x,y}(z) = \begin{cases} \eta(z) & z \neq x, y; \\ \eta(x) - 1 & z = x; \\ \eta(y) + 1 & z = y. \end{cases}$$

- Stationary measure $\mathbb{P}_\alpha = \nu_\alpha^{\otimes \mathbb{Z}^d}$ with $\nu_\alpha(n) = \frac{\alpha^n}{\sum_{j=0}^\kappa \alpha^j}$, $0 \leq n \leq \kappa$.

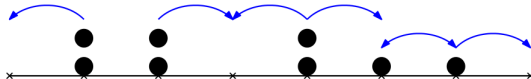


Figure: An illustration of GSEP with $\kappa = 2$.

Interacting particle systems

Example: Generalized symmetric exclusion process

- Empirical measure $\pi_t^N := N^{-d} \sum_{x \in \mathbb{Z}^d} \eta_{N^2 t}(x) \delta_{x/N},$
- Hydrodynamic limit $(\pi_t^N)_{t \geq 0} \xrightarrow{N \rightarrow \infty} (\rho_t)_{t \geq 0}$ with

$$\partial_t \rho_t = \nabla \cdot (D(\rho_t) \nabla \rho_t).$$

- Bulk diffusion matrix $D(\alpha) := \frac{\bar{\mathbf{a}}(\alpha)}{2\chi(\alpha)}, \chi(\alpha) := \text{Var}_\alpha[\eta(0)],$

$$p \cdot \bar{\mathbf{a}}(\alpha) p := \inf_{f \in C_0} \sum_{i=1}^d \mathbb{E}_\alpha [\mathbf{1}_{\{\eta(0)>0, \eta(e_i)<\kappa\}} (p_i + \nabla_{0,e_i} \Gamma_f(\eta))^2],$$

with f local function and $\Gamma_f(\tilde{\eta}) := \sum_{x \in \mathbb{Z}^d} \tau_x f(\tilde{\eta}).$

Interacting particle systems

- Particles seen as configuration $\mu_t = \sum_{i=1}^{\infty} \delta_{X_t^i} \in \mathcal{M}_{\delta}(\mathbb{R}^d)$.
- Diffusion matrix $\mathbf{a}_o : \mathcal{M}_{\delta}(\mathbb{R}^d) \rightarrow \mathbb{R}_{sym}^{d \times d}$
 - **locality:** \mathcal{F}_{B_1} -measurable;
 - **uniform ellipticity:** $|\xi|^2 \leq \xi \cdot \mathbf{a}_o(\mu) \xi \leq \Lambda |\xi|^2$.
 - **stationarity:** $\mathbf{a}(\mu, x) := \tau_x \mathbf{a}_o(\mu) = \mathbf{a}_o(\tau_{-x} \mu)$.
- $(X_t^i)_{t \geq 0}$ diffuses following $\nabla \cdot \mathbf{a}(\mu_t, X_t^i) \nabla$ in \mathbb{R}^d , where $\mathbf{a}(\mu_t, X_t^i)$ depends on the local configuration in $B_1(X_t^i)$.

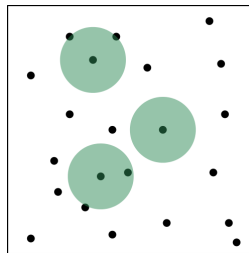


Figure: Each particle diffuses following the generator $\nabla \cdot \mathbf{a} \nabla$, where \mathbf{a} depends on the position and the local configuration around the particle.

Main result 3: Homogenization on particle systems

- Stationary measure \mathbb{P}_ρ as Poisson point process of density ρ .
- Finite volume approximation $\square_m = \left(-\frac{3^m}{2}, \frac{3^m}{2}\right)^d$,

$$p \cdot \bar{\mathbf{a}}(\square_m, \rho) p := \inf_{\phi \in \mathcal{H}_0^1(\square_m)} \mathbb{E}_\rho \left[\frac{1}{\rho|U|} \int_{\square_m} (p + \nabla \phi) \cdot \mathbf{a}(p + \nabla \phi) d\mu \right].$$

- Derivative $\partial_k f(\mu, x) := \lim_{h \rightarrow 0} \frac{1}{h} (f(\mu - \delta_x + \delta_{x+he_k}) - f(\mu))$.
- $\bar{\mathbf{a}}(\rho) = \lim_{m \rightarrow \infty} \bar{\mathbf{a}}(\square_m, \rho)$.

Theorem (Giunti, Gu, Mourrat, 2020)

$$|\bar{\mathbf{a}}(\square_m, \rho) - \bar{\mathbf{a}}(\rho)| \leq C 3^{-\alpha m}.$$

Proof: Subadditive quantity

- $\nu(U, p) = \inf_{\phi \in \mathcal{H}_0^1(U)} \mathbb{E}_\rho \left[\frac{1}{\rho|U|} \int_U \frac{1}{2} (p + \nabla \phi) \cdot \mathbf{a}(p + \nabla \phi) d\mu \right]$ is a subadditive quantity, i.e. $U = \sqcup_{i=1}^n U_i$,

$$\nu(U, p) \leq \sum_{i=1}^n \frac{|U_i|}{|U|} \nu(U_i, p).$$

- Observed in Dal Maso-Modica 86 for elliptic equation, and quantitative version in Armstrong-Smart 16 and developed in Armstrong-Kuusi-Mourrat 17.
- This renormalization approach now applies to various models: the finite-difference equations on **percolation clusters** (Armstrong-Dario 18, Dario 18, Dario-Gu 21), **the differential forms** (Dario 18), **the “ $\nabla \phi$ ” interface model** (Dario 19, Armstrong-Wu 19), **the Villain model** (Dario-Wu 20), **the Coulomb gases** (Armstrong-Serfaty 19).

Proof: Modified Caccioppoli inequality

- The classical Caccioppoli inequality for \mathbf{a} -harmonic function on \mathbb{R}^d

$$\int_{Q_r} |\nabla \tilde{u}|^2 \leq \frac{C}{r^2} \int_{Q_{3r}} |\tilde{u}|^2.$$

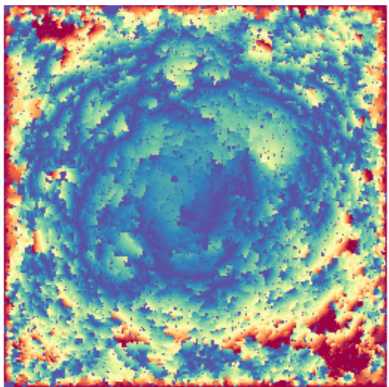
- The modified Caccioppoli inequality for particle systems:
 $\theta(d, \Lambda) \in (0, 1)$, such that for every u \mathbf{a} -harmonic function in Q_{3r}

$$\begin{aligned} & \mathbb{E}_\rho \left[\frac{1}{\rho|Q_r|} \int_{Q_r} \nabla(\mathbf{A}_{r+2}u) \cdot \mathbf{a} \nabla(\mathbf{A}_{r+2}u) d\mu \right] \\ & \leq \frac{C}{r^2 \rho |Q_{3r}|} \mathbb{E}_\rho [u^2] + \theta \mathbb{E}_\rho \left[\frac{1}{\rho|Q_{3r}|} \int_{Q_{3r}} \nabla u \cdot \mathbf{a} \nabla u d\mu \right]. \end{aligned}$$

- $\mathbf{A}_s u := \mathbb{E}_\rho[u | \mathcal{F}_{\overline{Q}_s}]$ and $(\mathbf{A}_s u)_{s \geq 0}$ has a L^2 -martingale structure.

Perspectives

- KMT coupling for random walk on percolation cluster.
- Heat kernel estimate for stable type random walk / long-range percolation.
- Optimal rate for hydrodynamic limit and fluctuation.
- Particles with more singular interactions.



Thank you for your attention.

感谢

Obrigado

Merci

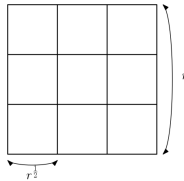
ありがとう

About effective coefficient \bar{a}

- Definition $p \cdot \bar{a}p = \mathbb{E}[(p + \nabla\phi_p)\mathbf{a}(p + \nabla\phi_p)]$.
- Representative volume method (REV): using the spatial average of the localized corrector

$$\mathbf{a}(\square_m)p := \frac{1}{|\square_m|} \int_{\square_m} \mathbf{a}(p + \nabla\phi_{p,m}), \quad \mathbf{a}(\square_m) \xrightarrow{m \rightarrow \infty} \bar{\mathbf{a}}.$$

- Complexity and precision: REV + reduction of variance, one gets a precision $r^{-\frac{d}{2}}$ with complexity of $O(r^{\frac{d}{2}})$ rounds of conjugate gradient method.



- Optimal complexity: proposed in Mourrat 16, precision $r^{-\frac{d}{2}}$ with complexity of $O(\log r)$ rounds of conjugate gradient method.

Classical methods

Monte-Carlo Markov chain

For the case $f = 0$, the solution of Dirichlet problem is $u(x) = \mathbb{E}_x[g(X_\tau)]$ for $(X_n)_{n \geq 0}$ the Markov chain associated to the operator $-\nabla \cdot \mathbf{a} \nabla$ and τ the hitting time of the boundary.

- **Advantages:** Dimension free, easy to program.
- **Disadvantages:** It takes time if we want $u(x)$ for **all** $x \in Q_r$.

Numerical experience: AHKM on elliptic equation

- $d = 2$, size = 128×128 , $\mathbf{a} \in \{\frac{1}{\sqrt{2}}, \sqrt{2}\}$ with law Bernoulli($\frac{1}{2}$).
- $f = 1$ and $g = 0$.
- $\lambda = 0.1$.
- The first 22 rounds of iteration give a convergence of errors
 $\varepsilon_n := \|f - (-\nabla \cdot \mathbf{a} \nabla u_n)\|_{L^2(Q_r)}$.

$$\begin{aligned}\{\varepsilon_n\}_{1 \leq n \leq 22} = & \{34.43, 18.56, 9.99, 5.38, 2.89, 1.56, 0.84, \\ & 0.45, 0.24, 0.13, 0.0709, 0.0382, 0.0206, \\ & 0.0111, 0.0059, 0.0032, 0.0017, 0.0009, \\ & 0.0005064, 0.0002730, 0.0001472, 7.94 \times 10^{-5}\}\end{aligned}$$

Numerical experience: AHKM on elliptic equation

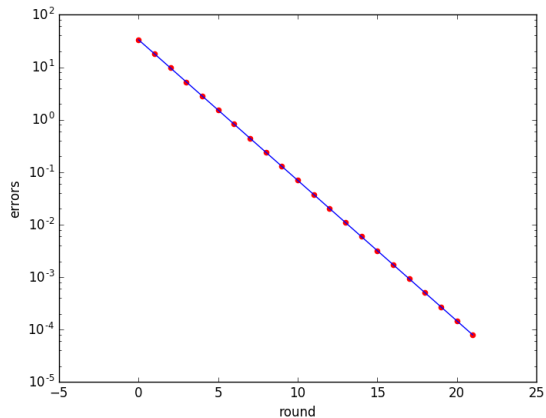


Figure: A numerical experience of the algorithm gives a very high precision of the solution.

Numerical experience: AHKM on percolation cluster

- $d = 2$, size = 256×256 , $p = 0.6$, $\mathbf{a} \in \{0\} \cup [0.5, 1]$, $\lambda = 0.1$.
- $-\nabla \cdot \mathbf{a} \nabla \phi_{e_1, L} = \nabla \cdot \mathbf{a} e_1$ with null boundary condition.
- This example **cannot** be captured by homogenized solution.
- Initial error $\varepsilon_0 = 1.12085310602$.

round	errors
1	0.0282597982969
2	0.0126490361046
3	0.00707540548365
4	0.00435201077274
5	0.00282913420116
6	0.00190945842802
7	0.00132483912845
8	0.000939101476657

Figure: A table of errors

Numerical experience: AHKM on percolation cluster

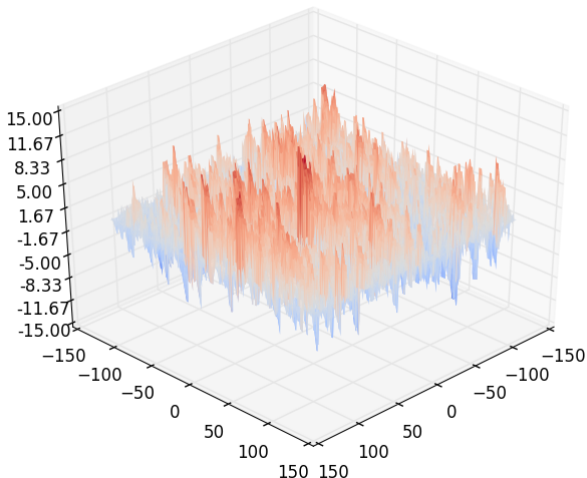


Figure: A simulation of the corrector on the maximal cluster of a cube 256×256 .

Equivalent definitions of $\bar{\mathbf{a}}$ for particle systems

The following two definitions are equivalent $\bar{\mathbf{a}}(\rho) = \tilde{\bar{\mathbf{a}}}(\rho)$.

- Finite volume approximation $\bar{\mathbf{a}}(\rho) = \lim_{m \rightarrow \infty} \bar{\mathbf{a}}(\square_m, \rho)$

$$\xi \cdot \bar{\mathbf{a}}(U, \rho) \xi := \inf_{\phi \in \mathcal{H}_0^1(U)} \mathbb{E}_\rho \left[\frac{1}{\rho|U|} \int_U (\xi + \nabla \phi) \cdot \mathbf{a}(\xi + \nabla \phi) d\mu \right],$$

- Using stationary gradient field

$$\begin{aligned} & \xi \cdot \tilde{\bar{\mathbf{a}}}(\rho) \xi \\ &:= \inf_{u \in \Gamma} \mathbb{E}_\rho [(\xi + \nabla u(\mu + \delta_0, 0)) \cdot \mathbf{a}(\mu + \delta_0, 0) (\xi + \nabla u(\mu + \delta_0, 0))] . \end{aligned}$$

where the function space Γ

$$\Gamma := \left\{ u : u = \int_{\mathbb{R}^d} \tau_x g(\mu) dx, \quad g \in \mathcal{C}_c^\infty(\mathbb{R}^d) \cap \mathcal{H}_0^1(\mathbb{R}^d) \right\}.$$